Effects of Overhangs on the Wind-Driven Rain Wetting of a Low-Rise Building

S. Sepehr M. Foroushani **Hua Ge, PhD, PEng** *Member ASHRAE* **David Naylor, PhD, PEng**

ABSTRACT

Wind-driven rain is known to be a major source of moisture loads on building envelopes and is responsible for numerous cases of building envelope failures. One of the classic solutions for preventing the building envelope from being extensively exposed to wind-driven rain is the use of overhangs. Previous studies have shown that the introduction of the overhang can change both the amount and the pattern of the wind-driven rain wetting of the facade significantly. In this work, the effects of overhangs on the distribution of wind-driven rain on the windward facade of a low-rise building are discussed based on the results of numerical simulations. It is shown that roof overhangs significantly reduce the amount of wind-driven rain deposition on the upper half of the facade. Wind speed is found to have a large influence on the protection that the overhang provides, while the intensity of rainfall does not have a significant effect. A physical explanation of the effects of overhangs is also presented.

INTRODUCTION

It was a rush of water leaks in multi-unit residential buildings in southern British Columbia during the early 1990s that drew attentions to the causes of such failures in buildings in Canada. Accordingly, a field survey conducted by the Building Envelope Research Consortium (BERC) confirmed that, rather than moisture from construction or condensation due to air leakage, rain penetration was the main source of the problem (Hazleden and Morris 1999). The field survey recognized the major concern to be poor design details and practice, not material quality or problems in maintenance (Hershfield 1996). Morris has mentioned "underestimation of wind-driven rain (WDR) and extended wetting" to be one of the causes of the problems in building envelopes, specifically in the regions with damp coastal weather (2006). One important finding was that the walls facing the prevailing wind directions had more problems in terms of moisture penetration (Hazleden and Morris 1999). In Europe too, WDR studies were first conducted in the regions with similar conditions in terms of climate. It is now well established that among different sources of moisture in buildings, WDR is the most critical, especially in climates like the costal climate of British Columbia, Canada.

Overhangs have been traditionally used for purposes including protection against rain. Nonetheless, the protective effect of roof overhangs against WDR wetting of building facades and its relation with the overhang configuration (sizing and geometry) are not clear to the designer. Consequently, design practice has been generally based on rule of thumb and is governed by the architectural expression. It is the objective of the present work to provide insight into the effectiveness of overhangs.

WDR studies usually consist of two main tasks: quantifying rain loads on the building facade and investigating the hygrothermal response of the envelope. There are different methods for quantification of WDR loads, namely, measurement, semi-empirical methods, and numerical simulation based on computational fluid dynamics (CFD). Due to its importance in the durability, evaluation of building envelopes and the proper design of envelopes, there have been quite a number of studies on quantifying WDR on building facades. However, it remains a difficult task to predict the distribution

S. Sepehr M. Foroushani is a graduate student and **David Naylor** is a professor in the department of Mechanical and Industrial Engineering, Ryerson University, Toronto and **Hua Ge** is an assistant professor in the department of Building, Civil, and Environmental Engineering, Concordia University, Montreal, Canada.

of WDR on buildings accurately, especially with the consideration of design details such as overhangs.

So far, measurements have been the primary tool of quantifying WDR. Nonetheless, as discussed by Blocken and Carmeliet, establishing a systematic experimental method for WDR quantification seems to be very difficult (2007). Different problems have been enumerated for WDR measurements, including that they can easily suffer from large error (Blocken and Carmeliet 2006), that they are time consuming and expensive, and that measurements on a particular building site would have restricted application in other cases (Blocken and Carmeliet 2007). Semi-empirical relationships correlating the quantity of WDR to the climatic parameters such as wind speed and direction and rainfall intensity have been developed. These correlations are generally simple and easy-to-use relations, but they can provide only rough estimations of the exposure of the building to WDR. As noted by Blocken and Carmeliet, with the drawbacks of measurements and semi-empirical methods on one hand, and the vast developments in CFD techniques and the computational power available to the engineer on the other hand, researchers have resorted to CFD-based numerical modeling techniques for quantifying WDR loads (2007).

A detailed review of WDR research is given by Blocken and Carmeliet (2004), where the pioneering work of Choi (1991) has been recognized as the starting point of the numerical research on WDR conducted in the past twenty years. In Choi's method, which is the basis of the present study, the raindrop trajectories are calculated based on a 3-D steady-state RANS (Reynolds-Averaged Navier Stokes) solution of the wind flow around the building using the standard k-ε turbulence model (1991; 1993). The spatial distribution of WDR on buildings is then determined based on the computed raindrop trajectories. This technique, which was originally applicable to steady wind and rain conditions only, has been extended by Blocken and Carmeliet (2000a, 2000b). In this extended method, a new weighted time-averaging technique allows the determination of both the spatial and temporal distribution of WDR.

Blocken and Carmeleit (2002) have studied a low-rise building of complex geometry under a few on-site recorded rain events. They also have made a "full-scale experimental verification" of the numerical method. As related to the subject of the present study, they have mentioned that for fixed wind speed and raindrop diameter the shelter effect of the overhang increases as the overhang width increases. In addition, the overhang has been reported to be less effective in sheltering the facade as the raindrop diameter decreases.

In the present work, based on the technique developed by Choi, the effectiveness of different overhangs on the wind-driven wetting of a low-rise building is investigated (1991; 1993). The effects of wind and rain conditions on the performance of the overhang are also examined. The local effects of the overhang and physical explanations for these effects have been the focus of discussion.

BUILDING GEOMETRY

A low-rise cubic building has been studied in this work. There are two reasons for choosing this simple geometry. First, there are published numerical studies in the WDR literature that provide a basis for validation of the present numerical simulations (Blocken 2004). Second, the simplicity of the building, and consequently the flow field around it, makes it easier and less time consuming to examine a number of different wind and rain conditions. In addition, it is expected that the effects of overhangs would be clearer and easier to assess on a simple building like this. The tested overhangs vary in width (OH), but they are all 15 cm thick and 10 m long.

Schematics of the cubic building, without and with an overhang, are shown in Figure 1. The building is subjected to undisturbed wind approaching normal to the windward facade with different speeds. An exponential profile, as described by Equation 1, is set for the approaching wind speed. Different rainfall intensities are studied under each wind condition. Three rectangular overhangs widths of 30 cm, 60 cm, and 90 cm are tested.

$$U(y) = U_H\left(\frac{y}{H}\right)^{\alpha} \tag{1}$$

In Equation 1, U is the velocity in x direction, y is the elevation from the ground, H is some reference height at which the reference velocity U_H is determined, and α is a profile exponent depending on the terrain type. A value of $\alpha = 0.15$, which represents an open terrain with little obstruction (Wieringa et al. 2001), and a reference height of $H = 10$ m are used in all the cases presented in the current study.

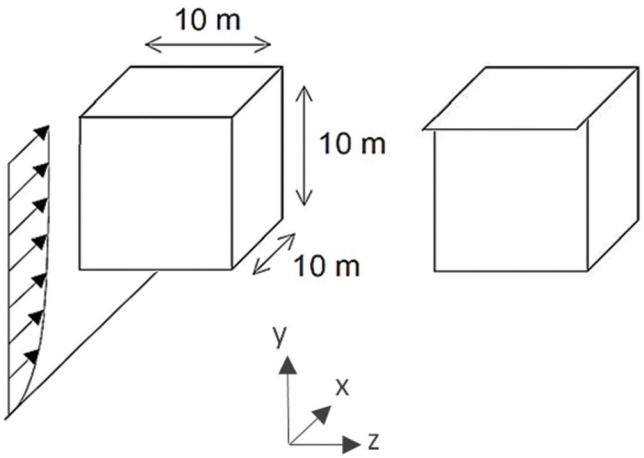

Figure 1 *LEFT: Cubic building subject to undisturbed exponential wind (Blocken 2004). RIGHT: The building with added overhang.*

Inlet turbulence kinetic energy and a modified dissipation rate are set at the inlet boundary based on the work of Blocken (2004) as

$$k = \frac{(u^*_{ABL})^2}{\sqrt{C\mu}} \quad (2)$$

and

$$\varepsilon(y) = \frac{(u^*_{ABL})^3}{\kappa(y + y_0)} \quad (3)$$

In these equations, y_0 is the aerodynamic roughness length and u^*_{ABL} is the friction velocity. Blokcen has computed different values for u^*_{ABL} based on measurements of the wind velocity profile (2004). A representative value of 0.69 m/s has been used in the current study. $C_\mu = 0.09$ is one of the constants of the k-ε model (Wilcox 1994). The more frequently used value of 0.42 has been used here for the Von Karman constant κ. Table 1 describes the boundary conditions of the present numerical simulations.

NUMERICAL SIMUILATION OF WDR

The commercial CFD code ANSYS FLUENT is used to solve the wind flow using the realizable k-ε turbulence model and standard wall functions. Standard interpolation for pressure and second order upwind discretization schemes for the momentum and turbulence equations are used. The SIMPLE method is selected for pressure-velocity coupling.

Figure 2 depicts a schematic of the computational domain with the building at the center of the bottom boundary. Information on the size and discretization of the domain are summarized in Table 2. A grid convergence study has been performed using three different grids based on the procedure proposed by the *Journal of Fluids Engineering* (ASME 2008). The area-averaged values of the pressure coefficient of the building have been used as the monitored field variable. The grid convergence index (GCI) has been shown to be substantially small (GCI ~5%).

The discrete phase model (DPM) module of FLUENT is utilized to perform the Lagrangian particle tracking and to compute the raindrop trajectories for a range of raindrop diameters. Trajectory data extracted from FLUENT for each diameter are further processed using a MATLAB code developed to calculate specific catch ratios. Catch ratio calculations are performed for 30 × 30 cm rectangular cells on the facade surface. These cells are the numerical representation of WDR gages. Finally, as discussed in the next section, these specific catch ratios are multiplied by the proper weighting function and integrated to yield the (total) catch ratio values.

The current approach is validated by comparison to the results of an earlier numerical study carried out by Blocken (2004). Details of the numerical solution are further discussed in a recent paper of Mohaddes Foroushani et al. (2012).

CATCH RATIO

Catch ratio is one of the main parameters used to describe the WDR loads on building facades quantitatively. By definition (Blocken 2004), catch ratio is the ratio of the WDR intensity on vertical surfaces (R_{wdr}) to the intensity of rainfall on the horizontal surface (the horizontal rainfall intensity, R_h), as given in Equation 4.

$$\eta(d, t) = \frac{R_{wdr}(d, t)}{R_h(d, t)} \quad (4)$$

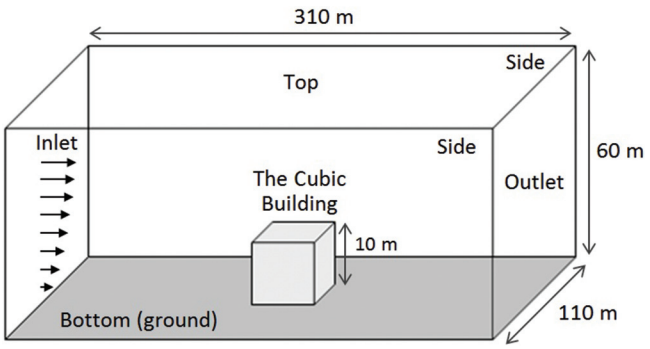

Figure 2 *The computational domain (not scaled).*

Table 1. Summary of the Boundary Conditions

Boundary		Inlet	Sides and Top	Bottom	Outlet	Building
Condition	Momentum	Normal to boundary U_{10} = 2, 5, 10 m/s α_p = 0.15	Symmetry	No slip, impermeable	Zero gauge pressure for backflow	No slip, impermeable
	Turbulence	k: Equation 2 : Equation 3		Roughness height (K_s = 0.03 m)	Backflow: k_{bf} = 1 m^2/s^2 $_{bf}$ = 1 m^2/s^3 (default values)	Roughness height (K_s = 0)
	DPM	—	—	Trap	—	Trap

In the case of a constant-intensity rainfall event and under steady-state wind flow conditions, the definition of the specific catch ratio may be rewritten as

$$\eta_d = \frac{A_h(d)}{A_f(d)} \tag{5}$$

In this equation, A_h is the area of a reference horizontal surface, R_{wdr} is the horizontal component of the rainfall flux vector (deposited on the vertical surface of the facade) and A_f is the wetted area on the building facade (Blocken 2004).

Integrated over the range of raindrop diameters that are likely to occur in a rainfall event, the parameter usually referred to as catch ratio is defined as

$$\eta = \int \eta_d f(d) dd \tag{6}$$

where the weighting function is the probability density function of each raindrop size (Best 1950).

RESULTS AND DISCUSSION

Three main parameters that are suspected to affect the effectiveness of the overhang are the overhang size, the wind speed, and the rainfall intensity. In this section, the effects of each factor are examined while the other two are fixed. Three rectangular overhangs with widths of 30, 60, and 90 cm are tested. Wind speeds of 2, 5 and 10 m/s representing low, moderate, and high-speed winds and rainfall intensities of 2, 5, and 10 mm/h are examined. Wind is approaching the windward facade in the normal direction in all the cases.

As mentioned previously, under steady-state wind and rain conditions, the calculation of catch ratio is simplified to calculating the ratio of areas from which raindrops are falling to the areas of the facade that are wetted by WDR. Therefore, raindrop trajectories and their deposition patterns on the facade play a key role in catch-ratio calculations. Hence, an understanding of the raindrop trajectories provides insight into the effects of overhangs too.

Two forces, namely gravity and drag, affect WDR drops. The balance between these forces determines the raindrop trajectory. Small raindrops (d < 2 mm) tend to be mainly affected by the wind drag force, more strictly follow the wind flow patterns, and thus have highly curved trajectories. On the other hand, large raindrops are gravity driven, are less influenced by the flow field, and tend to have straight trajectories. Their behavior has smaller deviation from free fall and their motion can be projected as vertically free falling under gravity at terminal (constant) velocity and horizontally being swept, without slip, by wind. Figure 3 shows the trajectories of small (d = 0.5 mm) and large (d = 3 mm) raindrops in side and top views. These graphs are generated for U_{10} = 5 m/s, but the trajectories follow similar patterns under different wind speeds.

The effect of overhangs on WDR deposition on buildings can be attributed to two major effects (Mohaddes Foroushani et al. 2012). The first is the direct protection of the facade from rain exposure. This effect is expected to be dominant in high rainfall intensities where large (gravity-driven) raindrops are more likely to appear along with lower speed winds. The second is the indirect effect, which is due to the disturbance introduced by the overhang in the wind flow pattern. This disturbance is pronounced especially in the standing upstream vortex, the high vorticity regions around the corners and edges, and the wake above the building roof. The indirect effect is expected to be more significant under low rainfall intensities where small (drag-driven) raindrops hold a greater share. The actual protecting influence of the overhang will be a combina-

Table 2. Computational Domain Size and Discretization

Domain Length (*x*)			310 m
Domain Height (*y*)			60 m
Domain Width (*z*)			110 m
Surface Mesh	Size	Domain sides	3 m
		Building walls	0.3 m
	Type		Quadrangle
Volume Mesh	Number of CVs		~6×10^5
	Type		Tetrahedral

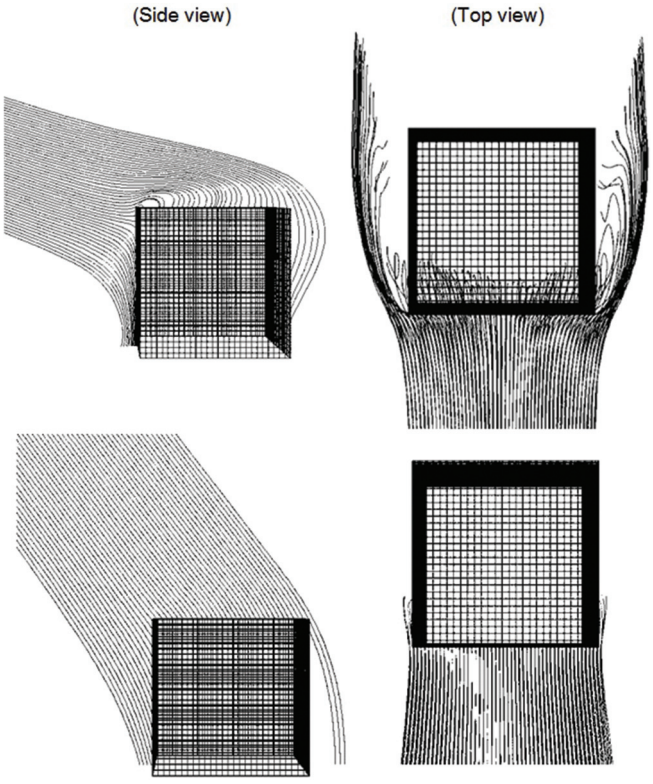

Figure 3 *Raindrop trajectories (U_{10} = 5 m/s), TOP: d = 0.5 mm, BOTTOM: d = 3 mm.*

tion of these two effects. Both these effects can be seen in Figure 4. Note that in addition to the few raindrops approaching the upper edge that are directly blocked by the overhang, others are also influenced by the presence of the overhang; the overhang has created a dead zone where raindrops have highly curved trajectories and approach the ground almost free falling. This is the indirect effect of the overhang.

Figure 5 shows the deposition patterns of 0.5 and 3 mm raindrops on buildings without an overhang and with a 60 cm overhang. Wind speed is fixed at U_{10} = 5 m/s. It can be seen

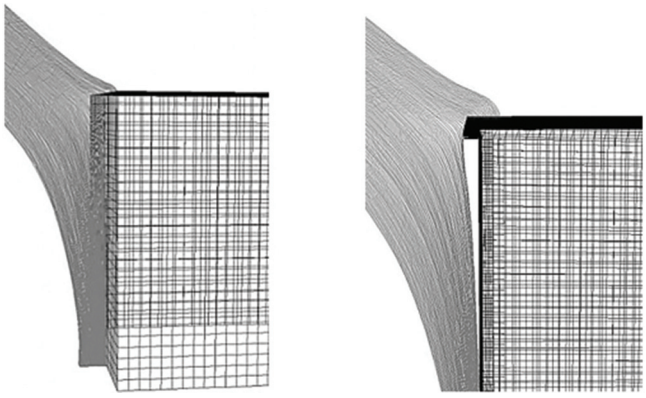

Figure 4 *Trajectories of 0.5 mm raindrops (*U_{10} *= 2 m/s) LEFT: No overhang, RIGHT: with 30 cm overhang.*

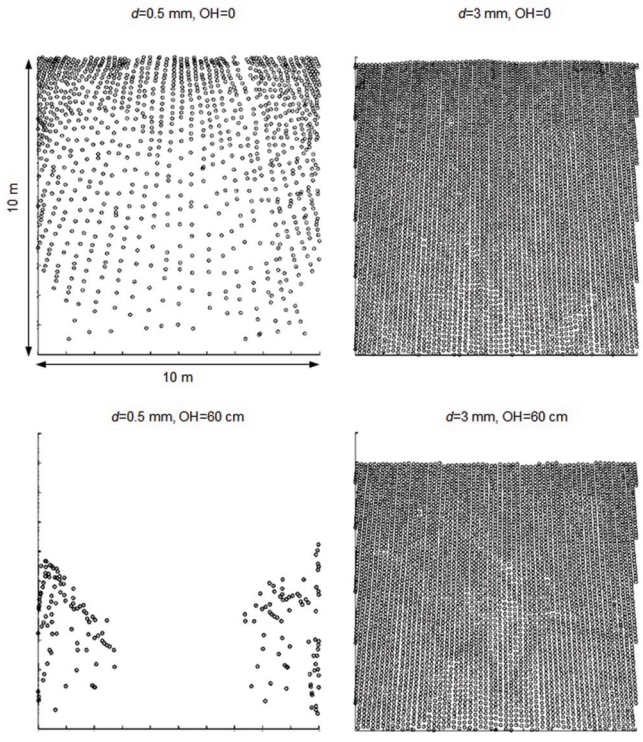

Figure 5 *Distribution of raindrops on the windward facade with no overhang (*U_{10} *= 5 m/s).*

that the small drag-dominant raindrops are driven towards the edges and corners. Therefore, corners and edges are subject to a higher concentration of WDR. The large gravity-dominant raindrops, on the other hand, are deposited on the facade more uniformly. There is, nonetheless, a higher concentration of WDR deposition at the upper edge of the facade. It can also be seen that the overhang almost completely protects the facade from smaller raindrops; only a few of these raindrops make it to the lower half of the facade near the edges and the upper half remain completely dry. On the other hand, only a small area at the top of the facade is protected from large raindrops by the direct shading effect that the overhang provides. The lower parts of the facade are almost not influenced at all.

Figure 6 shows the distribution of specific catch ratio on the facade for the same two raindrop sizes (0.5 and 3 mm), a fixed wind speed of U_{10} = 5 m/s, without and with a 60 cm overhang. It is observed that the introduction of overhangs not only changes the value of catch ratio at individual points, but also leads to changes in the wetting pattern of the facade (the configuration of the contour lines). The observations made based on the raindrop distribution are confirmed by these contours. Almost 40% of the facade is protected from 0.5 mm raindrops, for which no contour line is shown. Less than 10% of the facade is protected from 3 mm raindrop. The remainder of the upper half is also significantly, though not completely, protected. Specific catch ratio values (d = 3 mm) are reduced as much as 50% by introducing the 60 cm overhang.

Catch ratio contours for a wind speed of U_{10} = 5 m/s and a rainfall intensity of R_h = 5 mm/h are shown in Figure 7. Buildings with different overhang widths are compared to the building without an overhang. It can be seen that, under these wind and rain conditions, the wider overhangs provide much better protection at the upper half of the facade. A narrow strip beneath the upper edge of the facade has been fully protected from WDR after an overhang has been introduced. The height of this dry strip increases from almost 0.5 to around 2 m as the overhang width increases from 30 to 90 cm. On the other hand, the overhang has almost no effect on the lower half of the facade.

Figure 8 shows the distribution of total catch ratio on the windward facade under rainfalls with different intensities. These results are for a wind speed of U_{10} = 5 m/s. The results suggest that, with or without overhang, the rainfall intensity does not have a significant effect on wind-driven wetting of the facade. In addition, the performance of the overhang, at least at such moderate wind speeds, seems to be independent of the rainfall intensity. Under all the examined rainfall intensities, the top 15% region of the facade remains completely dry when the 60 cm is added to the building.

Finally, the effect of wind speed can be seen in the contours of Figure 9. In these contours, the rainfall intensity and the overhang width are fixed at 5 mm/h and 60 cm respectively. Wind speed seems to play a significantly larger role than the intensity of rainfall.

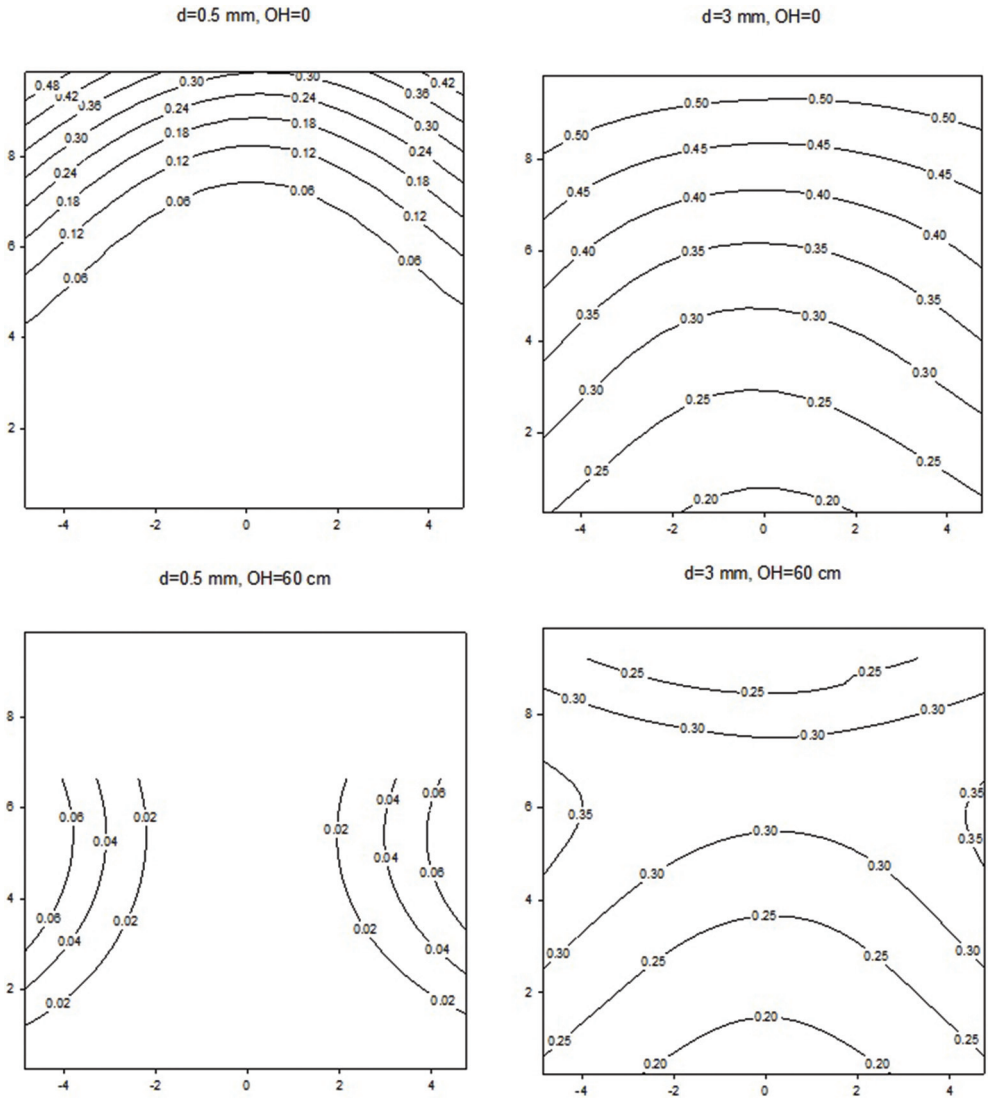

Figure 6 *Specific catch ratio contours on the windward facade (*U_{10} *= 5 m/s).*

The entire facade is exposed to considerably larger WDR loads under the high-speed wind of U_{10} = 10 m/s when compared to the low and moderate-speed winds. The effectiveness of the overhang also varies under different wind speeds. Based on these results, a 60 cm overhang reduces the WDR deposition on the upper half of the facade under low, moderate, and high wind speeds. Yet, in terms of relative protection with respect to the case without an overhang, the 60 cm overhang appears to be much more effective in the low-wind speed of U_{10} = 2 m/s. The percentage of the facade area fully protected by the 60 cm overhang reduces from approximately 25% under the U_{10} = 2 m/s wind to approximately 15% and 10% under 5 m/s and 10 m/s wind speeds respectively.

The slight deviation from fully symmetric wetting patterns that can be observed in the presented contours may be attributed to asymmetry in the flow field (especially for high wind speeds), numerical errors in the CFD solution of the wind flow, and the numerical errors associated with the catch ratio calculations and contour generation. Numerical tests at different grid levels have revealed that this asymmetric behavior is pronounced for coarser girds. It is therefore assumed to be mainly due to the numerical errors of the CFD solution.

CONCLUSION

The effects of roof overhangs on the wind-driven wetting of the windward facade of a low-rise building have been examined using numerical simulation. Three overhang widths were tested. The effects of wind speed and rainfall intensity on the performance of the overhangs are also studied. It is observed that the introduction of the overhang changes both the magnitude and the pattern of the WDR deposition on the facade. All the tested overhangs helped protect the upper half of the facade from WDR wetting under all the studied wind and rain conditions. The lower half of the facade, however, appears to be

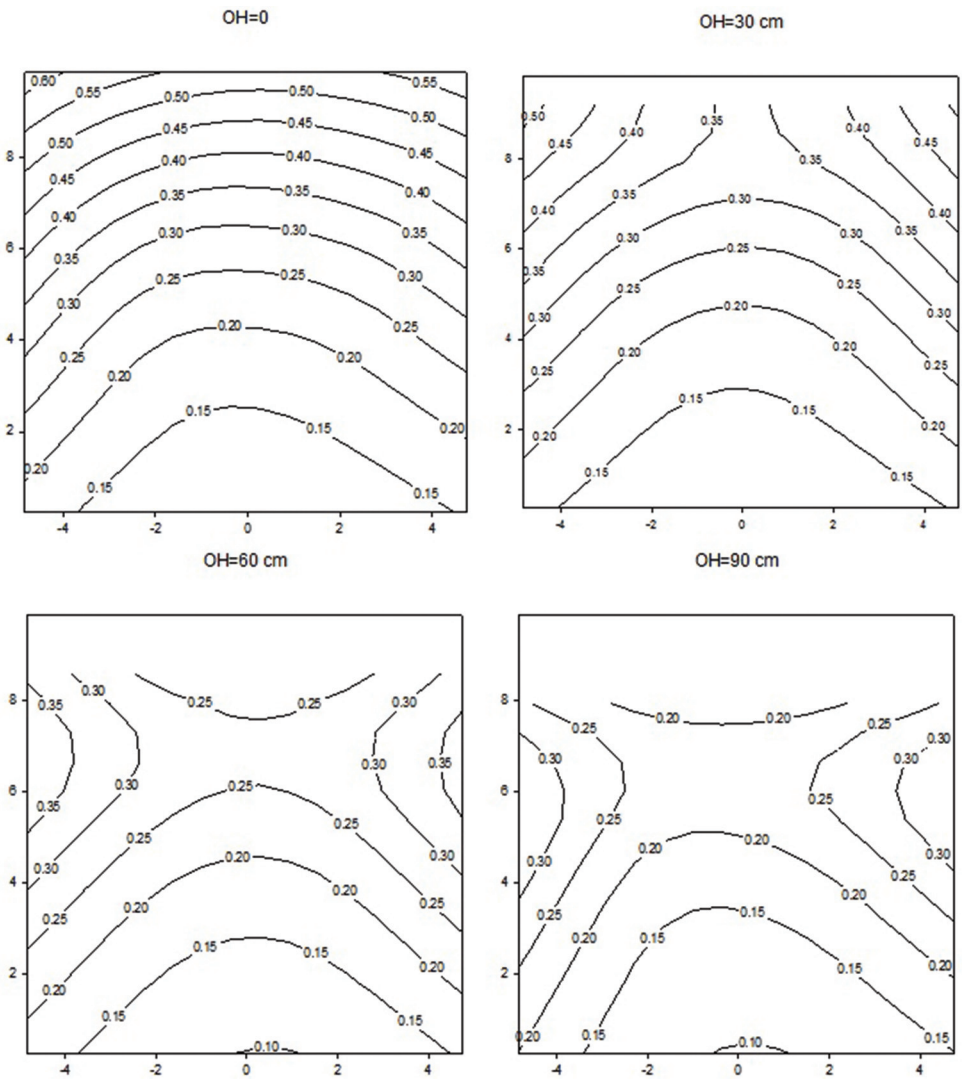

Figure 7 *Catch ratio contours on the windward facade with different overhangs (*U_{10}*=5 m/s,* R_h*=5 mm/h).*

almost not affected at all by the overhang. It is also shown that, compared to rainfall intensity, wind speed has a much larger influence on the WDR loads as well as the protection that the overhang can provide from these loads. The overhangs have significantly better protecting performances under low-speed winds.

FUTURE WORK

This work is part of a project that is intended to provide guidelines and recommendations on the design of overhangs that are effective in protecting building facades from large WDR loads. In order to achieve this, a number of other factors and cases must be further investigated in the future among which are different overhang shapes, (specifically pitched overhangs), realistic building geometries, and different wind angles. In addition, as is essential for any numerical study, results are to be compared with and validated by measured data collected from a number of test buildings.

ACKNOWLEDGMENTS

The authors would like to acknowledge the financial support of NSERC NEWBluidS Network, FP Innovations, and Ryerson University.

NOMENCLATURE

A_h	= reference horizontal area, m^2
A_f	= wetted area on facade, m^2
d	= raindrop diameter, mm
f	= raindrop diameter PDF (probability density function), 1/mm
H	= reference height, m
K_s	= surface roughness height, m
k	= turbulence kinetic energy, m^2/s^2
OH	= overhang width, cm
R_h	= rainfall intensity on the horizontal surface, mm/h

R_{wdr} = WDR intensity, mm/hr
t = time, s
U = wind speed, m/s
U_H = reference wind speed, m/s
u^*_{ABL} = friction velocity, m/s
y = vertical coordinate/ elevation from the ground, m
y_0 = aerodynamic roughness length, m
α = wind speed profile exponent, —
ε = turbulence dissipation rate, m^2/s^3
η = catch ratio, —
κ = von Karman constant, —

REFERENCES

ASME. 2008. Procedure for estimation and reporting of uncertainty due to discretization in CFD applications (Announcement). *Journal of Fluids Engineering* 130(7).

Best, A.C. 1950. The size distribution of raindrops. *Quarterly Journal of the Royal Meteorological Society* 76(327):16–36.

Blocken, B. and J. Carmeliet. 2000a. Driving rain on building envelopes—I: Numerical estimation and full-scale experimental verification. *Journal of Thermal Envelope and Building Science* 24(1):61–85.

Blocken, B., and J. Carmeliet. 2000b. Driving rain on building envelopes—II: Representative experimental data for driving rain estimation. *Journal of Thermal Envelope and Building Science* 24(2):89–110.

Blocken, B. and J. Carmeliet. 2002. Spatial and temporal distribution of driving rain on a low-rise building. *Civil Engineering* 5(5):441–62.

Blocken, B. 2004. Wind-driven rain on buildings. Doctoral. thesis, Katholieke Universiteit Leuven, Lueven, Belgium.

Blocken, B. and J. Carmeliet. 2004. A review of wind-driven rain research in building science. *Journal of Wind Engineering and Industrial Aerodynamics* 92(13):1079–1130.

Blocken, B. and J. Carmeliet. 2006. On the accuracy of wind-driven rain measurements on buildings. *Building and Environment* 41(12):1798–1810.

Blocken, B. and J. Carmeliet. 2007. Validation of CFD simulations of wind-driven rain on a low-rise building facade. *Building and Environment* 42(7):2530–2548.

Choi, E.C.C. 1991. Numerical simulation of wind-driven-rain falling onto a 2-D building. *Asia Pacific Conference on Computational Mechanics*, *Hong Kong*, 1721–28.

Choi, E.C.C. 1993. Simulation of wind-driven-rain around a building. *Journal of Wind Engineering and Industrial Aerodynamics* 46(47): 721-729.

Hazleden, D.G. and P.I. Morris. 1999. Designing for durable wood construction*: The 4 Ds, 8th International Conference On Durability Of Building Materials And Components*, Vancouver, Canada.

Foroushani, M.S.S., D. Naylor, and H. Ge. 2012. Numerical investigation of the effects of different overhang configurations on the wind-driven rain wetting of building facades. *Proceedings of ASME 2012 International Mechanical Engineering Congress & Exposition* (IMECE2012), Houston, Texas.

Morris, P.I. 2006. Damp coastal weather field issues and improving performance. *In Proceedings: Wood Protection*.

Hershfield, M. 1996. Survey of building envelope failures in the coastal climate of British Columbia. Research report for Canadian Mortgage and Housing Corporation, Ottawa, Canada.

Wieringa, J., A.G. Davenport, C.S.B. Grimoond, and T. R. Oke. 2001. New revision of davenport roughness classification. *The 3rd European and African Conference on Wind Engineering*, *Eindhoven, Netherlands.*

Wilcox, D. C. 1994. *Turbulence modeling for CFD*. California: DCW Industries.

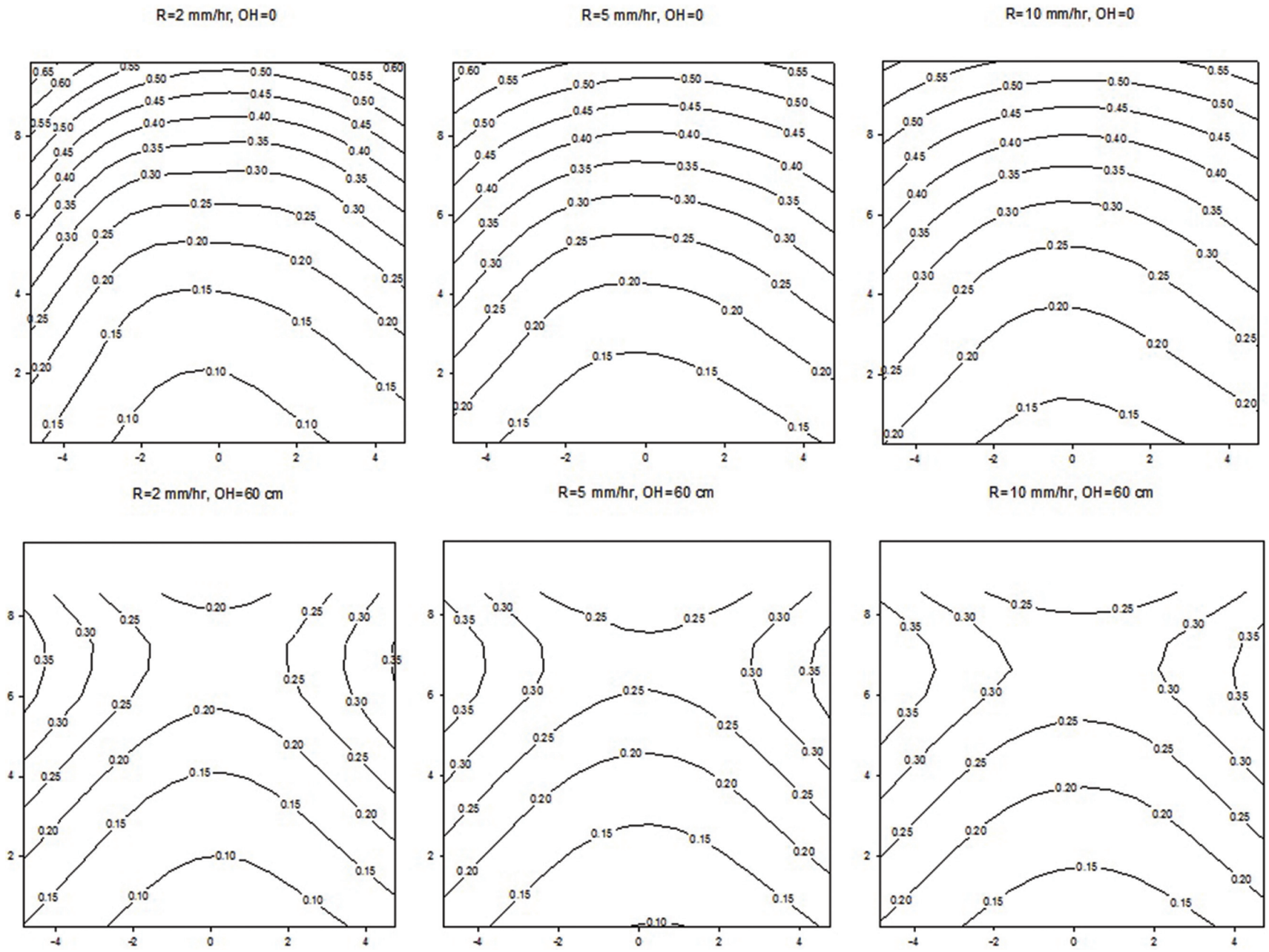

Figure 8 *Catch ratio contours on the windward facade under different rainfall intensities, without (TOP) and with (BOTTOM) 60 cm overhang (*U_{10}*=5 m/s).*

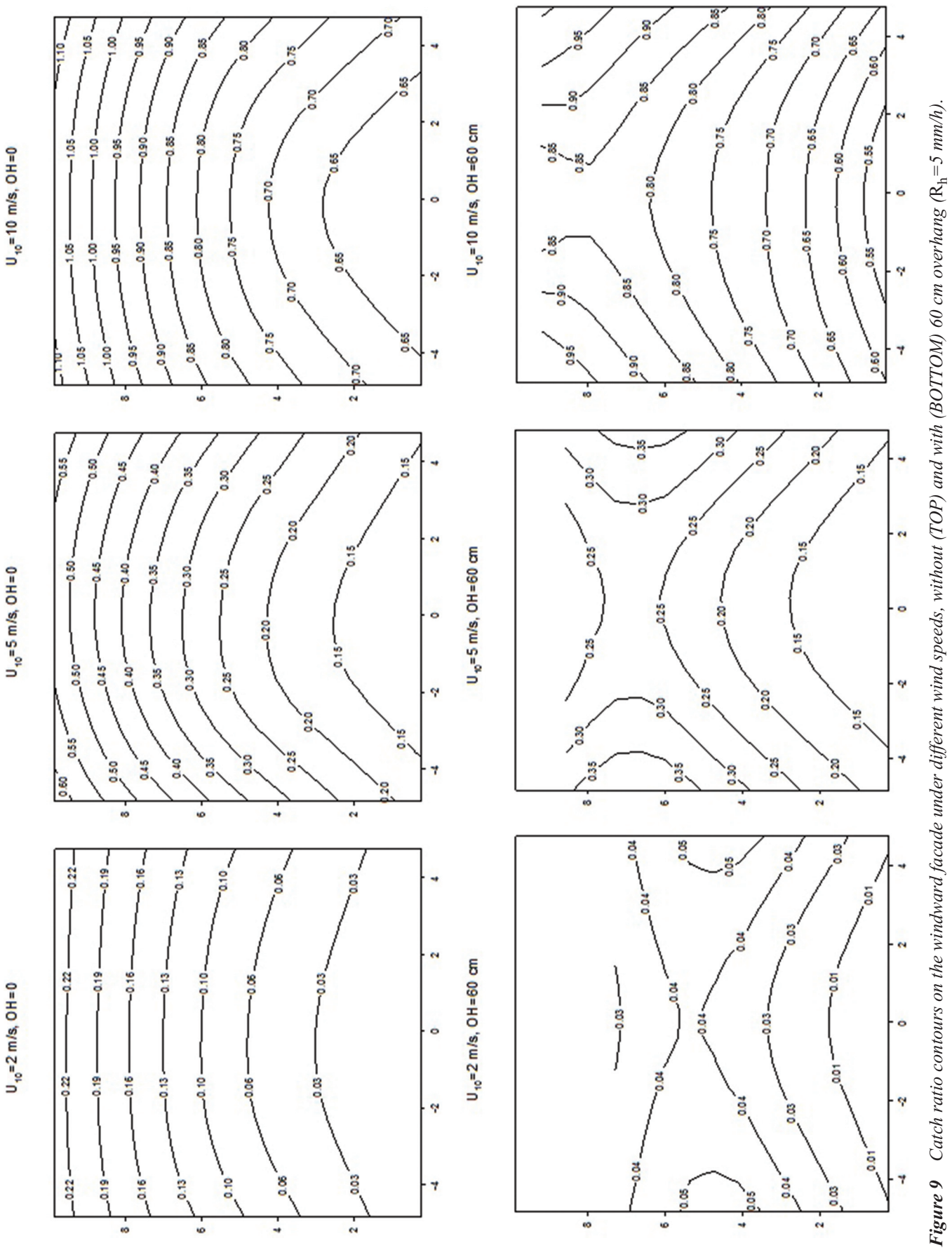

Figure 9 *Catch ratio contours on the windward facade under different wind speeds, without (TOP) and with (BOTTOM) 60 cm overhang (R_h=5 mm/h).*